

**Dibromine monoxide,  $\text{Br}_2\text{O}$ :**  
**the rotational spectrum and molecular properties**

Holger S. P. Müller and Edward A. Cohen

*Jet Propulsion Laboratory, California Institute **of** Technology*

*Mail Stop 183-301*

*Pasadena, CA 91109-8099*

## Abstract

The rotational spectra of  $^{79}\text{Br}_2\text{O}$ ,  $^{79}\text{BrO}^{81}\text{Br}$ , and  $^{81}\text{Br}_2\text{O}$  in their ground vibrational states as well as  $^{79}\text{BrO}^{81}\text{Br}$  in its  $\nu_2 = 1$  state have been studied in selected regions between 90 and 523 GHz. Transitions involving a large range of quantum numbers,  $6 \leq J \leq 12$  and  $0 \leq K_a \leq 12$ , have been observed permitting precise rotational and a large set of centrifugal distortion constants to be determined. All isotopic species as well as the excited state data were fit simultaneously. Ground-state effective and average structural parameters as well as an estimate of the equilibrium structure have been derived. The quartic distortion constants were used for a calculation of the harmonic force field. The complete quadrupole tensor has been determined. Its diagonalization reveals a largely covalent BrO bond with little  $\pi$ -bonding. The derived properties of  $\text{Br}_2\text{O}$  are compared with those of related compounds such as  $\text{Cl}_2\text{O}$ ,  $\text{IOBr}$ , and  $\text{HOCl}$ .

## 1. INTRODUCTION

Few bromine oxides are known, mainly because they are unstable at room temperature. Most of the limited spectroscopic and structural investigations were carried out in the solid state, " <sup>2</sup> Dibromine monoxide, Br<sub>2</sub>O, is comparatively well characterized. It was obtained in low yields by Zintl and Rieckner more than sixty years ago by passing Br<sub>2</sub> over 1 IgO as a not specified bromine oxide contaminated with unreacted bromine.<sup>3</sup> Using a solution of Br<sub>2</sub> in CCl<sub>4</sub>, Brenschede and Schumacher obtained higher yields dissolved in CCl<sub>4</sub> and identified it.<sup>4</sup> Pure Br<sub>2</sub>O was synthesized for the first time by Schwarz and Wiele as a decomposition product of a light yellow bromine oxide described as bromine dioxide.<sup>5</sup>

More recently, the Raman spectrum of solid Br<sub>2</sub>O at 77 K was recorded by Campbell *et al.* including <sup>16/18</sup>O isotopic shifts for the stretching fundamentals.<sup>6</sup> The symmetric stretching vibration  $\nu_1$ <sup>7</sup> or both stretching modes<sup>8,9</sup> were observed in Ar<sup>7,8</sup> or N<sub>2</sub> matrices<sup>9</sup> along with <sup>16/18</sup>O isotopic shifts. The structure of Br<sub>2</sub>O in the solid phase was studied by EXAFS (Extended X-ray Absorption Fine Structure) and very recently by single crystal X-ray diffraction.<sup>10</sup>

Very recently we have given a preliminary account on the investigations of the rotational spectra of Br<sub>2</sub>O and OBrO.<sup>11</sup> These have been the first high resolution studies and the first structure determinations of bromine oxides in the gas phase other than BrO. In this article the spectra of the three main isotopic species of Br<sub>2</sub>O and the fitting procedure are described in detail together with the derived spectroscopic constants and molecular properties.

## EXPERIMENTAL SECTION

**(a) Synthesis of  $\text{Br}_2\text{O}$ .**  $\text{Br}_2\text{O}$  was synthesized by passing  $\text{Br}_2$  through a column of yellow  $\text{HgO}$  at room temperature. The products were flowed through the microwave absorption cell at total pressures of 2-5 Pa. Although the yields were low, in agreement with earlier work,<sup>3</sup> many transitions could be observed with no or little signal averaging. This method has been used for most of the investigations.

During our studies of  $\text{OBrO}$ <sup>11</sup> it was discovered that  $\text{Br}_2\text{O}$  could be more readily observed as a secondary product of the  $\text{O} + \text{Br}_2$  reaction than as a product of the  $\text{Br}_2 + \text{HgO}$  reaction. Products of an oxygen discharge +  $\text{Br}_2$  were condensed on the wall of the absorption cell at -250 K.  $\text{OBrO}$  was evolved at *ca.* 250 K. At -260-270 K with pumping speeds adjusted to maintain pressures in the 0.5-2 Pa range, the  $\text{Br}_2\text{O}$  spectra became quite prominent. No effort has been made to characterize the solid product.

**(b) Spectrometer.** Details of the spectrometer have been given elsewhere.<sup>12</sup> The measurements were made employing a 1 m long, double-path coolable glass cell. Phase-locked klystrons (Varian) were used as sources, either on fundamental frequency (*ca.* 9061 Hz) with a diode detector, or at third to fifth harmonic using harmonic generators and a liquid He-cooled InSb hot electron bolometer as detector. Most of the measurements were done in the 383-4346117 and in the 312 - 322 GHz regions. Additional measurements were done at *ca.* 90 GHz and around 522 GHz.

## 11. R10S1JI.TS

**(a) Observed Spectra and Assignment.**  $\text{Br}_2\text{O}$  is a near symmetric prolate rotor ( $K \approx -0.9966$ ) with its dipole moment along the b-axis. The initial bond length of  $\text{Br}_2\text{O}$  was estimated to be 184-.3 pm from a comparison of ClO and BrO bond lengths in  $\text{Cl}_2\text{O}$ ,<sup>13</sup>  $\text{HOCl}$ ,<sup>14</sup> and  $\text{HOBr}$ .<sup>15</sup> This value is in agreement with 185 (1) pm from Ref. 9.1 The initial bond angle was taken from that study: 112 (2)°. Quartic distortion constants were derived from a force field calculation using the vibrational data from Refs. 6 and 8.

in the 412 to 434 GHz region studied first  ${}^1\text{R}_4$ ,  ${}^1\text{R}_5$ ,  ${}^1\text{Q}_6$ ,  ${}^1\text{P}_8$ , and  ${}^1\text{P}_9$  branches were predicted to be the strongest ones. Each branch was expected to have a characteristic quadrupole pattern which varied slowly with  $J$ . The observation of the  ${}^1\text{Q}_6$  branch for all three isotopomers near 412 GHz (see Fig. 1 for a detail of the  ${}^{79}\text{Br}_2\text{O}$  branch) and several members of the  ${}^1\text{R}_5$  and  ${}^1\text{P}_8$  branches permitted the unambiguous  $J$  assignment and the determination of rotational and diagonal quartic centrifugal distortion constants. The observation and assignment of selected transitions was then straightforward.

Using estimates of the vibration rotation interaction constants for the  $\nu_2 = 1$  state derived from  $\text{Cl}_2\text{O}$ ,<sup>13</sup> it was possible to identify one transition each of the  ${}^1\text{P}_8$  and  ${}^1\text{P}_9$  branches for the  ${}^{79}\text{BrO}{}^{81}\text{Br}$  isotopomer in the first excited bending mode in previously recorded spectra. Several other transitions were sought and found. No effort was made to assign other vibrational states of the mixed isotopomer or any excited state of the symmetric isotopomers. All rotational transitions used in the fits are in Table 1. The complete line list is available as supplementary material,

Both Br nuclei,  ${}^{79}\text{Br}$  and  ${}^{81}\text{Br}$ , have a spin of 3/2. Diagonal quadrupole coupling constants

were estimated using those of  $\text{Cl}_2\text{O}$ <sup>16</sup> scaled by the ratio  $eQq(\text{BrO})/eQq(\text{ClO})$ <sup>17,18</sup> and considering the slight change in bond angle. It was assumed that the z-quadrupolar axes coincide with the XO bonds.

Because of the two different Br nuclei each rotational transition of  $^{79}\text{BrO}^{81}\text{Br}$  consists of 16 strong quadrupole components with  $\Delta J = \Delta K$ . Both  $^{79}\text{Br}_2\text{O}$  and  $^{81}\text{Br}_2\text{O}$  have  $C_{2v}$  symmetry. Because of the spin-statistics levels with  $J$  odd or even are missing for transitions with  $K_a + K_c$  even or odd, respectively, reducing the number of strong hyperfine components to 6 or 10 respectively (see Figs. 2 and 3).

Transitions with higher  $J$  and  $K_a$  quantum numbers, which were among the first assigned, appear mostly as characteristic triplets for the  $C_{2v}$  species (Figs. 1 and 2) and as triplets or quartets for the mixed isotopomer.

At low  $J$  the quadrupole splittings are large and dominated by  $\chi_{aa}$ .<sup>19</sup> They can be rather complex (see Fig. 3). Because  $\chi_{-} (= \chi_{bb} - \chi_{cc})$  is large and of the same sign as  $\chi_{aa}$  the quadrupole splittings rapidly decrease with increasing  $J$  (see Fig. 1). At some intermediate  $J$  they are minimal and often unresolvable in the absence of other effects; this value of  $J$  increases with  $K_a$ . At even higher  $J$  the patterns spread out again because of the increasing effect of  $\chi_{-}$  (see Fig. 2).<sup>19</sup> Some transitions with large quadrupole splittings are given in Table 11,

The z-quadrupole axes are expected to be close to the BrO bonds which are not aligned with a principal inertial axis. Therefore, the off-diagonal quadrupole coupling constant  $\chi_{ab}$  is non-zero. Effects related to this constant occur as perturbations of the quadrupole patterns of near-degenerate levels with  $|\Delta J| \leq 2$ ,  $|\Delta K_a| = 1$ , and  $\Delta K_c$  even. Among the observed transitions the effects of  $\chi_{ab}$  are

particularly noticeable in the  $^1R_4$  branch and the  $^1R_5, J = 40$  transition of the mixed isotopomer because they would have unresolvable quadruple splittings in the absence of  $P_{ab}$ . In several cases complex patterns were observed as shown in Fig. 4. These are due to interactions between levels with  $\Delta J = 2, \Delta K_a = -1$  as shown in Fig. 5. The  $A_{J=1}$  resonances occur at higher  $J$ . They have been observed only for  $K_a = 4-3$  around  $J$  of 80 (see also Table 2). The near-degeneracies of such levels contribute most to the precise determination of  $\chi_{ab}$ , but more subtle effects of  $\chi_{ab}$  are widespread throughout the spectrum.

**(b) Fitting of the Spectra.** predictions and fittings were done with Pickett's program SPCAT and SPJU'1'20. Because of the two Br nuclei a symmetric coupling scheme was employed:  $I_1 + I_2 = I$ ,  $1-1 J = F$ . Spin statistics were taken into account for the two isotopomers with  $C_{2v}$  symmetry. Because  $I$  is not a "good" quantum number strong mixing can occur so that the assignment of an  $I$  value to a particular state is sometimes not obvious. In a number of cases, the small changes encountered in the course of the iterative fit would change the program's assignments during the fitting procedure. Particularly in the beginning, the resulting spectroscopic constants were substantially affected. In order to minimize these problems each transition for which the fitting program made multiple assignments was entered with all alternate assignments. A rejection criterion was chosen so that only one assignment would be included for each iteration.

The uncertainties attributed to the lines were in general one tenth of the half-width; they were increased for lines with low signal-to-noise ratio or incompletely resolved lines. The uncertainties

reflect a 20 confidence level. Blended lines were weighted according to their relative intensities.

The Hamiltonian is schematically described by

$$\mathcal{H} = \mathcal{H}_{\text{rot}} + \mathcal{H}_{\text{hfs}}$$

The rotational Hamiltonian is a Watson S reduction<sup>21</sup> in the  $1^+$  representation<sup>22</sup> and contains centrifugal distortion effects of up to eighths order. The hyperfine Hamiltonian includes nuclear Br quadrupole and spin-rotation effects as well as distortion terms for the diagonal quadrupole constants of the form  $[(\chi_J P^2 + \chi_K P_z^2), \mathcal{H}_Q]$ . All operators are defined positively, except  $D_J, D_{JK}$ , and  $D_K$  for reasons of tradition.

Values for each of the rotational constants are very similar among the isotopomers. However, it can be expected that the distortion constants are quite similar as well. However, some of the higher order constants showed initially isotopic variations much larger than expected. In order to extract the most information from the data set the spectroscopic constants were determined in a single, global, non-linear least-squares fit. A set of common constants was used for  $H_J, h_J$ , and the octic constants used in the fit. Some higher order constants ( $d_2$  and the remaining diagonal sextic constants) were constrained so that

$$C(81) = 2C(79,81) - C(79)$$

This relationship is quite good even when sufficient data is available to determine all three constants independently.

Each of the hyperfine constants were fixed together for all nuclei using the appropriate isotopic relationships taken from the Br atom.<sup>23</sup> It should be pointed out that for molecules where the quadrupole constants were determined very precisely, the isotopic ratios are very close to the atomic



value.<sup>24</sup> Because of the rotation of the principal axis system of the mixed isotopomer with respect to the symmetric ones its quadrupole tensor had to be adjusted. These corrections have been estimated from the structure and the quadrupole constants of the symmetric isotopomers. Corrections were not taken into account for the distortion parameters on the quadrupole constants and for the spin-rotation constants because the effects of the axis rotation for the mixed isotopomer were much smaller than the uncertainties of the respective constants.

The quadrupole constant  $\chi_{aa}$  was mostly determined by transitions with low  $J$  and  $K_a \geq 5$  while  $\chi_{\perp}$  was mostly determined by transitions with  $K_a \leq 4$  and rather high  $J$  (see Table 2). This may explain why the  $J$ -distortion on  $\chi_{\perp}$  and the  $K$ -distortion on  $\chi_{aa}$  were significantly determined. The inclusion of  $\chi_{aa}^K$  in the fit removed systematic deviations between calculated and observed quadrupole splittings at higher  $K_a$ 's.

initially the  $v_2 = 1$  state data was fit separately holding all ground state constants of  $^{79}\text{Br}_2\text{O}^{81}\text{Br}$  fixed and fitting those differences which seemed to be appropriate for the current set of transitions. Changes in the rotational and diagonal quartic distortion constants as well as  $H_K$  and  $\chi_{aa}$  were determined. Later the same molecular parameters were used in the combined fit.

Higher order parameters were kept in the fit if they reduced the standard deviation and did not introduce a high degree of correlation among the parameters. Some parameters with rather large uncertainties were retained although their effects on the quality of the fit were small. In such cases the uncertainties may be used to place reasonable limits on the magnitude of such terms and provide more realistic calculations of the uncertainties of other molecular parameters and the positions of unobserved lines. The particular choice of parameters has essentially no effect on the molecular para-

meters derived from the rotational and quartic distortion constants or from the quadrupole tensor. The magnitude from the K-dependent to the J-dependent and from the quartic to the octic distortion constants decrease rapidly and in a very regular way indicating that even the less well determined higher order parameters are of the right order of magnitude,

The spectroscopic constants of the ground and excited vibrational states are in Tables III and IV respectively. Statistics of the fit are in Table V.

**(c) Structural Parameters.** The  $\text{Br}_2\text{O}$  ground-state effective ( $r_0$ ) structure may be calculated from any two of the three moments of inertia or the  $a$  and  $b$  planar moments for each of the isotopic species. Table VI gives the  $r_0$  structure determined from a least-squares fit to the planar moments of all three isotopomers. The numbers in parenthesis represent the range of values when different choices of moments were used in the fit. Because the uncertainties of the rotational constants are very small, the structural parameters determined by either method are highly precise and agree among the isotopomers to more than the quoted figures. The accuracy of the structural parameters is entirely limited by vibrational effects.

The ground-state average ( $r_g$ ) structure was calculated from the  $B_g$  (Table VI). The harmonic contributions to the  $a$ -constants were calculated from the harmonic force field (*vide infra*) and subtracted off of the  $B_0$  to obtain the ground-state average rotational constants  $B_g$  (see Table VII). Because the inertial defects calculated from the ground state average rotational constants are smaller by a factor of 40 (ideally it should be zero) than those from the ground state effective constants, structural ambiguities are reduced by a similar amount. Isotopic differences in the  $r_g$  structure are

very small. For the bond length they are of the order of what can be derived from the formula below.

1 {equilibrium structural parameters can be estimated using an equation proposed by Kuchitsu:<sup>25</sup>

$$r_e = r_z - 3/2 a \langle u^2 \rangle + K.$$

where  $\langle u^2 \rangle$  and  $K$  are the zero-point mean square amplitude of the BrO bond and its perpendicular amplitude correction, respectively. The constant  $a$  is a Morse anharmonicity parameter,<sup>26</sup>  $1.976 \text{ \AA}^{-1}$ , derived from the BrO radical.<sup>17</sup> In this model differences between ground-state average and equilibrium bond angles are neglected. The estimate of  $r_e$  is also in Table VI together with structural data of related compounds. To allow a better comparison, the parameters of  $\text{Cl}_2\text{O}$  were calculated as described above for  $\text{Br}_2\text{O}$  using rotational constants of  $^{35}\text{Cl}_2\text{O}$  from Ref. 27, the harmonic force field from Ref. 13, and the Morse anharmonicity parameter  $2.201 \text{ \AA}^{-1}$ , of ClO, derived from Ref. 28.

The Br-Br substitution distance can be well determined: 305.87 pm, slightly smaller than the respective  $r_0$  and  $r_z$  values, but larger than the  $r_e$  value. Because of the small h-coordinate of the Br atoms (-9.47 pm) together with vibrational effects it is difficult to locate the O atom precisely without oxygen substitution.

**(d) Harmonic Force Field** calculations have been performed for  $\text{Br}_2\text{O}$  to obtain initial centrifugal distortion constants, to calculate a ground-state average structure and to estimate equilibrium structural parameters (*vide supra*), and to gain some insight into the bonding of this molecule. The computation was performed using Christen's NCA program.<sup>29</sup>

The stretching fundamentals have been observed in argon matrices.<sup>8</sup> Whereas neon matrix

wavenumbers usually are very close to gas phase values, those from other matrices can exhibit shifts of up to a few percent. In order to estimate gas phase harmonic wavenumbers, the symmetric and asymmetric stretching frequencies were scaled by 1.005 and 1.014, respectively. These values were derived from gas phase<sup>27</sup> and argon matrix<sup>30</sup> values for  $\nu_1$  and  $\nu_3$  of  $^{35}\text{Cl}_2\text{O}$ . These estimates of anharmonic gas phase wavenumbers were harmonized as described elsewhere,<sup>31</sup> using  $\omega/\nu = 1.020$  which was taken from a recent force field calculation of  $\text{HOBr}$ .<sup>15b</sup> Since no  $^{79,81}\text{Br}$  isotopic shifts were resolved, the frequencies were attributed to the  $^{79}\text{Br}^{16}\text{O}^{81}\text{Br}$  and  $^{79}\text{Br}^{18}\text{O}^{81}\text{Br}$  isotopomers, respectively, because the mixed isotopomers are the most abundant ones and their vibrational wavenumbers are very close to the average of the respective symmetric isotopomers.

Among the different types of input data the weights were chosen to reproduce all the input data in a satisfactory way. The input data were weighted inversely to the squares of their attributed uncertainties. A hundred times the experimental values were used for the quartic distortion constants,  $1\text{ cm}^{-1}$  and  $0.3\text{ cm}^{-1}$  for the vibrational wavenumbers and isotopic shifts, respectively, the experimental uncertainty was used for the  $V_2$  inertial defect difference.

The  $r_0$  structure has been used initially to describe the geometry of the molecule. The resulting force field was used to derive the  $r_e$  structure and to estimate the equilibrium structure (*vide supra*). This  $r_e$  structure was used in the final calculation. The resulting force constants with the potential energy distribution (PED) for the vibrational wavenumbers, results from an *ab initio* calculation, and experimental values for  $\text{Cl}_2\text{O}$  and  $\text{I}_2\text{O}$  are given in Table VII.1. A comparison of the input data with values calculated from the force field are given in Table IX.

## 111. DISCUSSION

**(a) Structure and Force Field.** The present force field reproduces the input data quite well. The differences between ground-state and equilibrium centrifugal distortion constants account for a substantial amount of the residuals (compare for example ground-state distortion constants with those of the excited bending mode, or see Ref. 15b for the case of DOBr). The residuals of the vibrational wavenumbers and their isotopic shifts may be due to perturbations in the matrix and the way the gas phase harmonic wavenumbers were approximated.

The solid state EXAFS data agree with the structural parameters of Br<sub>2</sub>O in the gas phase within the large EXAFS uncertainties ( $r = 185(1)$  pm,  $\alpha = 112(2)^\circ$ ).<sup>9</sup> However, a more recent single crystal X-ray diffraction study indicates larger structural differences between the solid and the gaseous states; two non-equivalent bonds of 185.7(5) and 187.5(5) pm and an angle of 114.2(2)° were found,<sup>10</sup>

The structural parameters and force constants of Br<sub>2</sub>O agree reasonably well with those from a high level *ab initio* calculation.<sup>32</sup> The overestimation of the bond length and the underestimation of the stretching force constants are fairly common for this type of calculation.

The estimated equilibrium structural parameters of Cl<sub>2</sub>O, derived from the ground-state average structure as described above, agree very well with those derived from equilibrium rotational constants (see Table V). The agreement is even better, when the latter is calculated from  $P_a$  and  $P_b$ . The small differences arise from the fact that the experimental equilibrium inertial defect is slightly different from zero. Thus it seems reasonable to assume that the estimate of the Br<sub>2</sub>O equilibrium structure

is a good one too.

There is an apparent trend in the force constants of  $X_2O$  compounds, and the differences in the diagonal force constants between  $F_2O$  and  $Cl_2O$  are much larger than those between  $Cl_2O$  and  $Br_2O$ , as expected. The stretching force constants  $f_r$  of  $Br_2O$  and  $Cl_2O$  are very similar; this may be related to the essentially pure single bond character of the  $XO$  bonds in these molecules.

The  $BrO$  bond in  $Br_2O$  is slightly larger than in  $HOBr$ , the situation is very similar for the  $ClO$  bonds in  $Cl_2O$  and  $HOCl$ . The increasing size of the  $X$  atom corresponds with an increasing bond angle in  $X_2O$  and  $HOX$  ( $X = Cl, Br$ ).

**(b) Hyperfine Constants.** The three independent parameters which describe the  $Br$  quadrupole tensor of  $Br_2O$  completely,  $\chi_{aa}$ ,  $\chi_{bb}$ , and  $\chi_{ab}$ , could be determined quite well, particularly in the global fit. Consequently, it has been possible to determine the orientation of the principal quadrupole axes with respect to the  $BrO$  bond. The  $z$ -axis of the quadrupole tensor is tilted  $2.4^\circ$  away from the  $BrO$  bond toward the other  $Br$  atom as shown in Fig. 6. The situation is quite similar to that reported recently for  $Cl_2O$ .<sup>13</sup> Although care is advised when ground- and excited-state quadrupole constants are combined, it is likely that the general conclusions for  $Cl_2O$  are not seriously affected, because vibrational effects on these constants are expected to be small with respect to the uncertainties.

From the principal components of the quadrupole tensor one can calculate the ionic,  $i_c$ , and  $\pi$ -characters,  $\pi_c$ , of the  $XO$  bond in  $Br_2O$  and  $Cl_2O$ .<sup>19, 22</sup> The results are shown in Table X together with those of related compounds. In both  $X_2O$  molecules have essentially covalent  $XO$  bonds with almost negligible contributions from  $\pi$ -back bonding. The ionic characters derived in this way are

in line with the view that the XO group (X = halogen) is only slightly more and the Br atom less electronegative than the Cl atom.

It should be noted that in the absence of a good measurement of  $\chi_{ab}$  the usual assumption that the z-quadrupole axis coincides with the chemical bond would lead to a significant error in the calculation of  $\chi_z$  and  $\chi_x$ . For a nearly cylindrical y symmetric bond

$$\frac{\Delta \chi_x}{\chi_x} \approx \frac{2\Delta \chi_z}{\Delta \chi_z} \approx \frac{3\cos 2\theta_{za}}{2\cos 2\theta_{ra}}$$

where  $\theta_{za}$  is the angle between the z- and the a-axis and  $\theta_{ra}$  is the angle between the bond and the a-principal axis. The  $\Delta$ 's refer to the errors introduced in the respective constants. For the present case  $\Delta \chi_x/\chi_x \approx 30940$  and  $\Delta \chi_z/\chi_z \approx 15\%$ . For  $\text{Cl}_2\text{O}$  these errors lead to estimates of the ionic and n-contributions of 0.35 and 0.08 respectively.<sup>16</sup> Similarly one would derive values of 0.48 and 0.12 for  $\text{Br}_2\text{O}$ . It is noteworthy that in both cases the n-electrons would be in the molecular plane, increasing the ionic character due to the o-bond. These ionic characters are larger than those of  $\text{ClF}$  and  $\text{BrF}$  respectively, see Table X. This is rather unusual considering that fluorine is the most electronegative element and the fact that the ionic character of a given bond should depend on the electronegativity of the atoms or atom groups involved.

Two quadrupole distortion terms have been determined significantly. For a rather rigid molecule one would expect the ratios  $\chi_{aa}^K/\chi_{aa}$  and  $\chi^-/\chi$  to be of the order of  $-D_K/A$  and  $4d_1/(B-C)$ . Thus  $\chi_{aa}^K$  and  $\chi^-$  should be of the order of -17.5 and -0.58 kHz, respectively, for the  $^{79}\text{Br}$  nucleus, close to the experimental values of -29.4 (26) and -0.520 (94) kHz.

In contrast to the quadrupole coupling constants, the spin-rotation coupling constants of  $\text{Br}_2\text{O}$  are not particularly well determined. The spin-rotation constants of  $\text{Br}_2\text{O}$  can be used to estimate the paramagnetic shielding  $\sigma_p^{(\text{Br})}$  at the Br nucleus:<sup>37</sup> *ca.* -3650 ppm; because of the relatively large uncertainties of the spin-rotation constants that value has to be viewed cautiously. The absolute value is close to that of  $\text{BrI}^+$  (*cu.* -3700 ppm)<sup>24</sup> and  $\text{BrNO}$  (*ca.* -3770 ppm),<sup>38</sup> somewhat larger than that of  $\text{IOBr}$  (*ea.* -2490 ppm),<sup>34</sup> but much larger than that of  $\text{HBr}$  (-513 ppm).<sup>39</sup> Thus, it can be concluded that the spin-rotation coupling constants of  $\text{Br}_2\text{O}$  obtained in this study are of the right order of magnitude.

#### IV. CONCLUSION

The first high resolution study of  $\text{Br}_2\text{O}$  has been performed in the millimeter and submillimeter regions. Precise spectroscopic constants have been obtained for  $^{79}\text{Br}_2\text{O}$ ,  $^{79}\text{BrO}^{81}\text{Br}$ , and  $^{81}\text{Br}_2\text{O}$  in the ground vibrational states and for the mixed isotopomer in the first excited bending mode permitting structural parameters and the harmonic force field to be determined. It has been shown that the determination of the off-diagonal quadrupole coupling constant  $\chi_{ab}$  is crucial to diagonalize the quadrupole tensor properly and to derive ionic and  $n$ -contributions.



## ACKNOWLEDGMENT

We would like to express our gratitude to Dr. H. M. Pickett for customizing his programs and some helpful comments and to Prof. K. Seppelt for communicating results prior to publication. H. S. P. M. thanks the National Research Council for a NASA-NRC Resident Research Associateship during this research. This research was performed at the Jet Propulsion Laboratory, California Institute of Technology, under a contract with the National Aeronautics and Space Administration.

## References

- <sup>1</sup>R P .Wayne, G. Poulet, P. Biggs, J.P. Burrows, R. A. Cox, P. J. Crutzen, G. D. Hayman, M. E. Jenkin, G. Le Bras, G. K. Moortgat, U. Platt, R. N. Schindler, *Atmos. Envir.* 29,2677 (1995).
- <sup>2</sup><sub>M</sub> W. Chase, *J. Phys. Chem. Ref. Data* **25**, 1069 (1996).
- <sup>3</sup>E. Zintl and G. Rienäcker, *Ber. Dtsch. Chem. Ges. B* **1930**, 63, 1098.
- <sup>4</sup><sub>w</sub> Brenschede and H. J. Schumacher, a) *Z. Phys. Chem. (Leipzig)* **B29**, 356 (1935); b) *Z. Anorg. Allg. Chem.* 226, 370(1936).
- <sup>5</sup>R. Schwarz and H. Wiele, a) *Naturwissenschaften* 26, 742 (1938); b) *J. Prakt. Chem.* 152, 157 (1939).
- <sup>6</sup>C. Campbell, J. P.M. Jones, and J. J. Turner, *Chem. Commun.* 888 (1968).
- <sup>7</sup>I. E. Tevault, N. Walker, R. R. Smardzewski, and W. B. Fox, *J. Phys. Chem.* 82,2733 (1978).
- <sup>8</sup>S. I). Allen, M. Poliakoff, J. J. Turner, *J. Mol. Struct.* 157, 1 (1987).
- <sup>9</sup>W. Levason, J. S. Ogden, M. D. Spicer, and N. A. Young, *J. Am. Chem. Soc.* 112, 1019 (1990).
- <sup>10</sup>I Hwang, R Kuschel, and K. Seppelt, submitted to *Z. Anorg. Allg. Chem.*
- <sup>11</sup>H S P Müller, C. E. Miller, and E. A. Cohen, *Angew. Chem.* 108, 2285 (1996); *Angew. Chem. Int. Ed. Engl.* **35**, 2129 (1996).
- <sup>12</sup>R. R. Friedl, M. Birk, J. J. Oh, and E. A. Cohen, *J. Mol. Spectrosc.* 170, 383 (1995).
- <sup>13</sup>M Sugie, M. Ayabe, H. Takeo, C. Matsumura, *J. Mol. Struct.* 352/353, 259 (1995).
- <sup>14</sup>R M. Escribano, G. Di Leonardo, L. Fusina, *Chem. Phys. Lett.* 259, 614 (1996).
- <sup>15</sup>(a) E. A. Cohen, G. A. McRae, 'I'. L. Tan, R. R. Friedl, J. W. C. Johns, and M. Noël, *J. Mol. Spectrosc.* 173,55 (1995); (b) E. A. Cohen, H. S. I'. Müller, 'I'. L. Tan, G. A. McRae, J. W. C. Johns,

and M. Noël, to be submitted.

<sup>16</sup>R. H. Jackson and D.J. Millen, in *Advances in Molecular Spectroscopy*, edited by A. Mangini, Vol. III (Pergamon Press, Oxford, 1962), p. 1157.

<sup>17</sup>(a) E. A. Cohen, H. M. Pickett, and M. Geller, *J. Mol. Spectrosc.* 87,459 (1981 ); H. S. P. Müller and E. A. Cohen, to be submitted.

<sup>18</sup>E. A. Cohen, H. M. Pickett, and M. Geller, *J. Mol. Spectrosc.* 106,430 (1984).

<sup>19</sup>C. H. Townes and A. L. Schawlow, *Microwave Spectroscopy* (Dover, New York, 1975),

<sup>20</sup>H. M. Pickett, *J. Mol. Spectrosc.* 148,371 (1991).

<sup>21</sup>J. K. G. Watson, *J. Chem. Phys.* 46, 1935 (1967).

<sup>22</sup>W. Gordy and R. L. Cook, *Microwave Molecular Spectra*, 3rd ed. (Wiley, New York, 1984).

<sup>23</sup>H. H. Brown and J. G. King, *Phys. Rev.* 142, 53 (1966).

<sup>24</sup>H. S. P. Müller and M. C. L. Gerry, *J. Phys. Chem.* 103, 577 (1995).

<sup>25</sup>(a) K. Kuchitsu, *J. Chem. Phys.* 49,4456 (1968); K. Kuchitsu, T. Fukuyama, and Y. Merino, *J. Mol. Struct.* (b) **1**, 463 (1968); (c) 4,41 (1969).

<sup>26</sup>K. Kuchitsu and Y. Merino, *Bull. Chem. Soc. Jpn.* 38, 805 (1965),

<sup>27</sup>Y. Xu, A. R. W. McKellar, J. B. Burkholder, and J. J. Orlando, *J. Mol. Spectrosc.* **175**, 68 (1996).

<sup>28</sup>J. B. Burkholder, P. D. Hammer, C. J. Howard, A. G. Maki, G. Thompson, and C. Chackerian, Jr., *J. Mol. Spectrosc.* 124, 139 (1987).

<sup>29</sup>D. Christen, *J. Mol. Struct.* 48, 101 (1978).

<sup>30</sup>(a) M. M. Rochkind and G. C. Pimentel, *J. Chem. Phys.* 42, 1361 (1965); (b) H. S. P. Müller and H. Willner, unpublished results.

<sup>31</sup>H. S. P. Müller and H. Winner, J. Phys. Chem. 97, 10589 (1993).

<sup>32</sup>T. J. Lee, J. Phys. Chem. **99**, 15074 (1995).

<sup>33</sup>T. Saarinen, E. Kauppi, and L. Halonen, J. Mol. Spectrosc. 142, 175 (1990).

<sup>34</sup>Y. Koga, H. Takeo, S. Kondo, M. Sugie, C. Matsumura, G. A. McRae, and E. A. Cohen, J. Mol. Spectrosc. 138, 467 (1989).

<sup>35</sup>A. C. Legon and J. C. Thorn, Chem. Phys. Lett. 215, 554 (1993).

<sup>36</sup>B. Fabricant and J. S. Muentz, J. Chem. Phys. 66, 5374 (1977).

<sup>37</sup>(a) N. F. Ramsey, *Molecular Beams* (Oxford University, London, 1956); (b) Ch. Schlier, Fortschr. Phys. 9, 455 (1961); (c) W. H. Flygare, J. Chem. Phys. 41, 793 (1964).

<sup>38</sup>C. Degli Esposti, F. Tamassia, and G. Cazzoli, J. Mol. Spectrosc. 163, 313 (1994).

<sup>39</sup>A. H. Saleck, T. Klaus, S. P. Belov, and G. Winnewisser, Z. Naturforsch. A 51, 898 (1996).

**TABLE I:** Rotational transitions<sup>a</sup> of Br<sub>2</sub>O used in the fits.

	ground state			$v_2 = 1$ <sup>79</sup> BrO <sup>81</sup> Br
	<sup>79</sup> Br <sub>2</sub> O	<sup>79</sup> BrO <sup>81</sup> Br	<sup>81</sup> Br <sub>2</sub> O	
<sup>1</sup> Q <sub>0</sub>		56		
<sup>3</sup> P <sub>1</sub>	39		40	
<sup>1</sup> Q <sub>1</sub>	19 <sup>l</sup>	19 <sup>l</sup>		
<sup>1</sup> R <sub>2</sub>	78 <sup>u</sup>	55 <sup>u</sup> , 79 <sup>u</sup>	80 <sup>u</sup>	
<sup>1</sup> P <sub>2</sub>		26 <sup>u</sup>		
<sup>1</sup> R <sub>3</sub>	34 <sup>l,u</sup> , 60 <sup>u</sup> , 61 <sup>l</sup> , 62 <sup>l</sup> , 69 <sup>u</sup>	35 <sup>l,u</sup> , 601 <sup>l</sup> , 62 <sup>u</sup> , 63 <sup>l</sup> , 64 <sup>l</sup> , 791	351 <sup>u</sup> , 621 <sup>u</sup> , 631 <sup>l</sup> , 641 <sup>l</sup> , 71 <sup>l</sup> , 75 <sup>u</sup> , 77 <sup>l</sup> , 80 <sup>l</sup> , 87 <sup>l</sup>	33 <sup>l,u</sup> , 34 <sup>l</sup> , 351 <sup>l</sup> , 36 <sup>l</sup>
<sup>1</sup> R <sub>4</sub>	45 <sup>u</sup> , 46 <sup>l</sup> , 471 <sup>u</sup> , 481 <sup>u</sup> , 51 <sup>u</sup> , 53 <sup>l,u</sup>	46 <sup>l,u</sup> , 47 <sup>l</sup> , 481 <sup>u</sup> , 491 <sup>l</sup> , 51 <sup>l</sup> , 54 <sup>u</sup>	47 <sup>l,u</sup> , 48 <sup>l,u</sup> , 49 <sup>l,u</sup> , 54 <sup>l,u</sup> , 55 <sup>l</sup>	471 <sup>u</sup> , 481 <sup>u</sup> , 491 <sup>u</sup> , 53 <sup>u</sup>
<sup>1</sup> R <sub>5</sub>	23, 27-30	27-30, 64 <sup>l,u</sup>	14, 23, 24, 24, 28-31	25, 27, 28
<sup>1</sup> R <sub>6</sub>	6	6, 40	6	
<sup>1</sup> Q <sub>6</sub>	25, 34-37, 40, 45-59, 87 <sup>u</sup> , 88 <sup>l</sup> , 911 <sup>u</sup> , 93 <sup>u</sup> , 111 <sup>l</sup> , 112 <sup>l</sup> , 1141 <sup>l</sup> , 1161, 1181, 121 <sup>l</sup> , 123 <sup>u</sup>	29, 30, 37, 38, 50-52, 59, 60, 84 <sup>l,u</sup> , 1121, 1131, 1141 <sup>l</sup> , 115 <sup>u</sup> , 1161 <sup>u</sup> , 1171, 119 <sup>u</sup> , 120 <sup>u</sup> , 121 <sup>l</sup>	7-14, 16-24, 28-41, 105 <sup>l</sup> , 1061, 1081 <sup>l</sup> , 110 <sup>l</sup> , 111 <sup>u</sup> , 112 <sup>l,u</sup> , 115 <sup>l</sup> , 117 <sup>l,u</sup> , 119 <sup>u</sup> , 1 <sup>l</sup> , 120 <sup>l</sup> , 121 <sup>u</sup>	45, 47, 52, 54, 55, 57
<sup>1</sup> P <sub>6</sub>	36	36, 38	37	36
<sup>1</sup> P <sub>7</sub>	21, 24, 32, 61	24, 33, 60	19, 33, 61, 62	62, 63
<sup>1</sup> P <sub>8</sub>	40, 41, 47, 48, 57	40-42, 47-49	41, 42, 49, 58	43-46, 50
<sup>1</sup> P <sub>9</sub>	64, 72, 80, 81, 82	65, 66, 71, 77, 82, 83	65, 66, 71-73, 82-84	67, 72, 73
<sup>1</sup> P <sub>10</sub>	92, 93	54, 89, 90, 97	90, 91, 98	
<sup>1</sup> P <sub>11</sub>		121		

<sup>a</sup> in symmetric top notation. <sup>l, u</sup> lower and upper KC, respectively, of the lower state.

**TABLE 11:** Observed frequencies (MHz) and assignments<sup>a</sup> of selected rotational transitions with large quadrupole splittings, uncertainties<sup>b</sup>(kHz), and residuals (kHz) (o-c) of Br<sub>2</sub>O.

Isotopomer	$J_{Ka,Kc} - J_{Ka',Kc'}$	C	
$I, I'' - I', I''$	obs. freq.	uric.	o-c
<sup>81</sup> Br <sub>2</sub> O	156, -145,	$\chi_{aa}$	
3,16-3,15	388795.566	50	24
0,15-0,14	388796.813	120	36
3,15-3,14	388797.263	120	-26
1,14-1,13	388798.278	50	-21
2,13 - 2,12	388807.580	50	-16
2,14-2,13			
2,16-2,15			
3,14-3,13			
1,16-1,15			
2,17-2,16			
3,13-3,12	388810.769	70	3
3,18-3,17	388816.909	80	29
2,15-2,14	388818.222	60	-13
1,15-1,14			
3,12-3,11	388819.749	80	-42
<sup>81</sup> Br <sub>2</sub> O	17, - 6,	$\chi_{aa}$	
3,5 -3,4	431048.334	100	-32
3,7 -3,6	431049.319	80	-30
1,6- 1,5	431051.593	50	-2
3,6- 3,5	431055.045	80	28
0,7- 0,6			
3,8 -3,7	431056.731	60	-11
1,8- 1,7	431059.165	100	-5
3,4 -3,3	431060.802	60	38
2,5 -2,4			

2,6- 2,5			
2,9- 2,8			
2,8- 2,7			
1,7- 1,6	431066,426	70	-58
2,7 -2,6			
3,9- 3,8	431067.341	100	21
3,10 -3,9	431070.3	50	-6

<sup>79</sup> Br <sub>2</sub> O	40., <sub>40</sub> -39,,39	x-	
2,40-0,39	90757.144	25	12
2,41-2,40	90781.817	25	-12
2,42-2,41	90783.336	25	-5
2,39-2,38			
2,38-2,37			
0,40-2,39	90808.148	40	7

<sup>81</sup> Br <sub>2</sub> O	41 0,41-401,40	x-	
3,42-3,41	90859.569	20	7
3,41-3,40	90859.938	30	-4
3,40-3,39	90860.260	30	14
3,43-3,42	90878.834	30	14
1,42-1,41	90880,650	30	-12
1,40-1,39	90881.669	30	-o
3,39-3,38	90882.424	30	-14
3,44-3,43	90900.97s	40	-15
1,41-1,40	90902.422	30	-8
3,38-3,37	90903.897	30	-12

<sup>79,R</sup>111r20      79<sub>4,76</sub> - 78<sub>3,75</sub>      x-, (x<sub>ab</sub>)

77<sub>4,73</sub> - 78<sub>3,75</sub> = 4063 MHz

3,82-3,81	418562.770	300	96
1,79-1,78	418563.295	90	-100
0,79-2,78			

3,76-3,75	418563.838	200	-233
1,80-1,79	418579.500	100	117
3,77-3,76			
2,81-2,80	418581.041	75	-82.
1,78-2,77			
2,80-2,79	418582.500	150	-56
3,81-3,80	418583.497	70	68
2,77-2,76			
2,78-1,77	418584.647	60	1
3,78-3,77	418598.881	80	-74
3,80-3,79	418601.998	60	11

$^{79/81}\text{Br}_2\text{O}$   $80_{3,77-792>78}$   $\chi_{-}, \chi_{ab}$

$80_{3,77-794,75} = 2732 \text{ MHz}$

3,79-3,78	412123.002	80	22
3,80-3,79	412124.194	150	-18
2,78-2,77	412168.595	80	-10
2,79-2,78	412169.412	80	6
1,81-1,80	412173.000	60	22
3,82-2,81	412174.249	60	-30
1,79-1,78	412178.295	50	-15
3,77-3,76	412222.086	50	-2

$^{79}\text{Br}_2\text{O}$   $525,47-514,48$   $\chi_{ab}$

$54_{4,51} - 52_{5,47} = 417 \text{ MHz}$

2,51-2,50	425858.447	80	-24
2,54-2,53	425865.497	70	22
2,53-2,52	425874.634	60	-13
0,52-0,51	425877.021	65	-14
2,52-2,51	425885.018	75	16
2,50-2,49	425897.373	70	21



$^{81}\text{Br}_2\text{O}$	565,52-554,5,	$\chi_{\text{ab}}$	
$53_{5,49} - 55_{4,51} = 874 \text{ MHz}$			
3,59-3,58	432454.813	400	-71
3,58-3,57	432455.846	150	60
1,55-1,54			
1,57-1,56			
3,57-3,56			
1,56-1,55	432459.612	90	-11
3,56-3,55	432461,986	120	26
3,53-3,52	432464.130	120	29
3,54-3,53	432466.154	120	5

<sup>a</sup>For blended lines frequencies, uncertainties and residuals are given only for the first hyperfine components, only  $J$  and  $F'$  assignments for the remaining components. Components not observed or not used in the fit have been omitted. For transitions affected by  $\chi_{\text{ab}}$  the perturbing levels and energy differences are also given.

<sup>b</sup>20 confidence level.

**TABLE III:** Spectroscopic constants' (MI Iz) and inertial defect (amu Å<sup>2</sup>) of Br<sub>2</sub>O in the ground vibrational state.

	<sup>79</sup> Br <sub>2</sub> O	<sup>79</sup> BrO <sup>81</sup> Br	<sup>81</sup> Br <sub>2</sub> O
Rotational constants			
$A - (B + C)/2$	31879.7770 (66)	31857.985 S (48)	31836.1153 <b>(79)</b>
$(B + C)/2$	1340.84020 (33)	1324.56744 (28)	1308.32641 (42)
$(B - C)/4$	13.732064 (48)	13.416095 (32)	13.104093 (46)
$A$	33220.6172 (64)	33182.5530 (47)	33144.4417 (76)
$B$	1368.30433 (29)	1351.39963 (30)	1334.53459 <b>(36)</b>
$C$	1313.37607 (39)	1297.73525 (28)	<b>1282.11822 (48)</b>
Inertial defect			
$A^2$	0.234085 (1 87)	0.234149 (163)	0,234195 (246)
Quartic centrifugal distortion constants			
$D_J \cdot 10^4$	2.85030 (82)	2.78410 (80)	<b>2.71842 (90)</b>
$D_{JK} \cdot 102$	<b>-1.913650 (264)</b>	-1.891064 (238)	-1.868525 (231)
$D_K$	1.051 317(126)	1.048704 (96)	1.046052 (151)
$d_1 \cdot 10^5$	-1.96723 (124)	-1.90199 (119)	<b>-1.83822(121)</b>
$d_2 \cdot 10^7$	-3.5330 (291)	-3.3658 (151)	<b>-3.1986(291)</b>
Sextic centrifugal distortion constants			
$H_J \cdot 10^{11}$	6.84 (60)	6.84 (60)	<b>6.84 (60)</b>
$H_{JK} \cdot 10^9$	4.487 (167)	4,422 (159)	<b>4.356 (167)</b>
$H_{KJ} \cdot 106$	-2.535 (41)	-2.493 (38)	<b>-2.450 (41)</b>
$H_K \cdot 10^4$	1.1680(109)	1.1622(103)	<b>1.1564(109)</b>
$h_1 \cdot 10^{13}$	1.793 (99)	1.793 (99)	<b>1.793 (99)</b>
Octic centrifugal distortion constants			
$l_{JK} \cdot 10^{12}$	-6.59 (1 69)	-6.59 (169)	<b>-6.59 (169)</b>
$l_{KKJ} \cdot 10^{10}$	7.34 (1 92)	7,34 (192)	<b>7.34 (192)</b>
$l_K \cdot 10^*$	-2.62 (47)	-2.62 (47)	<b>-2.62 (47)</b>

Nuclear quadruple coupling constants and quartic distortion terms<sup>c</sup>

$\chi_{aa}$	551.119(196)	-0.987 0.821	461,232 (164)
$\chi_{aa}^{J''} 10^4$	2.0 (21)		1,7(18)
$\chi_{aa}^{K'} \cdot 10^2$	<b>-2.93 (20)</b>		-2.45 (17)
<b>x-</b>	<b>405.361 (208)</b>	<b>0.995</b> <b>-0.814</b>	338.633 (174)
$\chi_{-}^{J''} 10^4$	-5.20 (94)		-4.34 (79)
<b>x-K'' 10</b>	<b>1.5 (23)</b>		1.2(19)
$ \chi_{ab} ^d$	<b>613.112(333)</b>	<b>0.503</b> <b>0,422</b>	512.185 (279)

Nuclear spin-rotation constants<sup>e</sup>

$C'_{aa} \cdot 10^3$	42.1 (63)		45.3 (67)
$C'_{bb} \cdot 10^3$	8.4 (24)		9.1 (26)
$C'_{cc} \cdot 10^3$	11.3 (26)		12.2 (28)

<sup>a</sup> Numbers in parentheses are two standard deviations in units of the least significant figures. Watson's S reduction was used in the representation 1'.

<sup>b</sup> One common constant for all three isotopomers was used for each of  $H_J$ ,  $h_J$ ,  $I_{JK}$ ,  $I_{KKJ}$ , and  $I_K$ ;  $d_2$ ,  $H_{JK}$ ,  $H_{KJ}$ , and  $H_K$  were constrained so that  $C(81) = 2 C(79,81) - C(79)$ ; see text.

<sup>c</sup> Upper (lower) values for  $^{79}\text{Br}$  ( $^{81}\text{Br}$ ) nucleus of  $^{79}\text{Br}_2\text{O}$  ( $^{81}\text{Br}_2\text{O}$ ), isotopic ratios fixed. Values for  $^{79}\text{BrO}^{81}\text{Br}$  are differences from the values of the respective nucleus for the symmetric isotopomer due to the rotation of the principal axis system; see also text.

<sup>d</sup>  $\text{sig}\{\chi_{ab}(\text{Br}_1)\} = -\text{sig}\{\chi_{ab}(\text{Br}_2)\}$ ;  $\text{sig}(\Delta\{\chi_{ab}(\text{Br}_1)\}) = \text{sig}(\Delta\{\chi_{ab}(\text{Br}_2)\})$

**TABLE IV:** Spectroscopic constants (MHz) and inertial defect (amu Å<sup>2</sup>) of <sup>79</sup>BrO<sup>81</sup>Br in the first excited bending mode.<sup>a</sup>

parameter	$v_2 = 1$	$(v_2 = 1) - v_0$
Rotational constants		
$A - (B + C)/2$	32084.7968 (161)	226.8113 (164)
$(B + C)/2$	1323.51311 (82)	-1.05433 (85)
$(B - C)/4$	13.47581 (114)	0.059 72(1 14)
$A$	33408.3099 (154)	225.7570 (1 56)
$B$	1350.46473 (198)	-0.934 89(1 96)
$C$	1296.56149 (280)	-1.17376 (283)
Inertial defect		
$\Delta_2$	0.43073 (136)	0.19658 (137)
[centrifugal distortion constants		
$D_J \cdot 104$	2.769 70(1 10)	-0.01441 (102)
$D_{JK} \cdot 102$	-1.899923 (318)	-0.008859 (1 89)
$D_K$	1.092927 (289)	0.044223 (284)
$H_K \cdot 104$	1.2379 (168)	0.0757 (137)
Qu		

TABLE V: Statistics of the fit.

	ground state			$v_2 = 1$
	$^{79}\text{Br}_2\text{O}$	$^{79/81}\text{Br}_2\text{O}$	$^{81}\text{Br}_2\text{O}$	$^{79/81}\text{Br}_2\text{O}$
total number of observed rotational transitions	76	72	96	30
total number of observed lines	156	192	245	76
number of lines with $0 \leq \text{residual} < 10$ ,	116	141	191	52
$1 \sigma \leq \text{residual} < 2 \sigma$ ,	30	37	47	17
$20 < \text{residual} < 3 \sigma$ ,	5	5	6	6
$3 \sigma \leq \text{residual} < 6 \sigma$	5	5	1	1

**TABLE VI:** Structural parameters (pm, deg) of Br<sub>2</sub>O and related compounds.

para- meter	Br <sub>2</sub> O <sup>a</sup>				HOBr <sup>b</sup>
	$r_0$	$r_z$	$r_e^c$	$r_e$	$r_e$
$r(\text{BrO})$	184.29 (20)	184.333 (5)	183.786		182.798
$\angle(\text{BrOX})$	112.24 (20)	112.249 (5)	112.249		102.99
	Cl <sub>2</sub> O <sup>d</sup>			<sup>e</sup>	HOCl <sup>f</sup>
	$r_0$	$r_z$	$r_e^c$	$r_e$	$r_e$
$r(\text{ClO})$	170.13	170.189	169.563	169.59	168.897
$\angle(\text{ClOX})$	110.89	110.914	110.914	110.88	102.965

<sup>a</sup> This work, for uncertainties see text. <sup>b</sup> Ref. 15. <sup>c</sup> Estimate from  $r_z$ , *scc* text.

<sup>d</sup> This work, rotational constants from Ref. 27. <sup>e</sup> Ref. 13. <sup>f</sup> Ref. 14.

**TABLE VII:** Ground state average rotational constants (Ml Iz) of Br<sub>2</sub>O.

parameter	<sup>79</sup> Br <sub>2</sub> O	<sup>79</sup> BrO <sup>81</sup> Br	<sup>81</sup> Br <sub>2</sub> O
$A_z$	32969,925	32932.482	32894.994
$B_z$	<i>1367.0458</i>	1350.1624	1333.3184
$C_z$	1312.6012	1296.9699	1281.3624

**TABLE VII 1:** Force constants ( $\text{Nm}^{-1}$ ) of dihalogen monoxides and potential energy distribution (PED)<sup>a</sup> of  $\text{Br}_2\text{O}$ .

para- meter	$\text{Br}_2\text{O}$		$\text{Cl}_2\text{O}$	$\text{F}_2\text{O}$	PED		
	exptl. <sup>b</sup>	<i>ab initio</i> <sup>c</sup>	exptl. <sup>d</sup>	exptl. <sup>e</sup>	$\nu_1$	$\nu_2$	$\nu_3$
$f_r$	287.4	253.9	294.9	410.5	0.858	0.084	1.131
$f_b$	102.3	108.3	123.7	147.1	0.265	0.786	
$f_{rr}$	33.4	31.6	50.4	86.0	0.100		-0.131
$f_{rrr}$	28.3	26.6	31.2	22.1	-0.223	0.120	

<sup>a</sup>For  $^{79}\text{BrO}^{81}\text{Br}$ ; only contributions  $\geq 0.03$  are given. <sup>b</sup>1<sup>st</sup> this work.

<sup>c</sup>CCSD(T)/TZ2P values from Ref. 32 <sup>d</sup>Ref. 13 <sup>e</sup> Ref. 33



TABLE IX: Comparison of experimental spectroscopic constants' ( $\text{cm}^{-1}$ , kHz,  $\text{amu } \text{\AA}^2$ ) with those calculated from the force field.

para- meter	$^{79}\text{Br}_2\text{O}$		$^{79}\text{BrO}^{81}\text{Br}$		$^{79}\text{Br}^{18}\text{O}^{81}\text{Br}$		$^{81}\text{Br}_2\text{O}$	
	ohs.	C-o <sup>b</sup>	ohs.	C-o <sup>b</sup>	ohs.	C-oh	ohs.	C-o <sup>b</sup>
$(\Delta) \nu_1$		0.90	539.4	-2.3	-26.4	1.31		-0.89
$(\Delta) \nu_2$		1.50		177.6		-0.98		-1.51
$(\Delta) \nu_3$		0.76	644.7	7.5	-33.0	0.46		-0.77
$D_J$	0.2850	0.0044	0.2784	0.0010		0.2760	0.2718	-0.0022
$D_{JK}$	-19.14	-0.45	-18.91	-0.34		-17.01	-18.69	-0.21
$D_K$	1051	-23	1049	-25		828.9	1046	-25
$10^3 d_1$	-19.67	-0.34	-19.02	0.01		-20.80	-18.38	0.33
$10^3 d_2$	-0.353	0.030	-0.337	0.035		-0.366	-0.32	0.038
$\Delta\Delta_2$		0.2025	0.1966	0.0040		0.2259		0.1987

<sup>a</sup>  $\nu_i$  for  $^{79}\text{BrO}^{81}\text{Br}$ ;  $\Delta \nu_i := \nu_i(\text{Br}_2\text{O}) - \nu_i(^{79}\text{BrO}^{81}\text{Br})$  eke.

<sup>b</sup> Calculated value minus observed value: equal to the calculated value if no observed value is given.

TABLE X: Quadruple coupling constants and derived parameters of  $^{79}\text{Br}_2\text{O}$  in comparison to related molecules.

parameter	$^{79}\text{Br}_2\text{O}^{\text{a}}$	$\text{HO}^{79}\text{Br}^{\text{b}}$	$^{79}\text{Br}^{35}\text{Cl}^{\text{c}}$	$^{79}\text{BrF}^{\text{d}}$	$^{35}\text{Cl}_2\text{O}$	$^{35}\text{ClF}^{\text{e}}$
$\chi_{\text{aa}} / \text{MHz}$	552.119 (196)	915.663	875.078	1086.892	-71.45 <sup>f</sup>	-145.872
$\chi_{\text{bb}} / \text{MHz}$	-73.379 (138)	-448.905	-437.539	-543.446	6.86 <sup>f</sup>	72.936
$\chi_{\text{cc}} \equiv \chi_{\text{y}} / \text{MHz}$	-478.740 (149)	-466.758	-437.539	-543.446	64.59 <sup>f</sup>	72.936
$ \chi_{\text{ab}}  / \text{MHz}$	613.112(333)	20.4	0	0	-82. <sup>g</sup>	0
$\chi_{\text{z}} / \text{MHz}$	927.64 (46)	915.97	875.078	1086.892	-123. <sub>2</sub>	-145.872
$\chi_{\text{x}} / \text{MHz}$	-448.90 (47)	-449.21	-437.539	-543.446	58. <sub>6</sub>	72.936
$\eta_{\text{z}}$	0.03217 (53)	0.0192	0	0	0.05	0
$\theta_{\text{za}} / \text{deg}$	31.4869 (77)	0.86			32.2 <sup>g</sup>	
$\text{em} / \text{deg}$	33.87	2.01			34.6 <sup>g</sup>	
$i_{\text{c}}$	0.108	0.109	0.080	0.342	-0.048	0.305
$\pi_{\text{c}}$	0.025	0.014			-0.036	

<sup>a</sup> This work. <sup>b</sup> Ref. 34. <sup>c</sup> Ref. 35. <sup>d</sup> Ref. 24. <sup>e</sup> Ref. 36. <sup>f</sup> Ref. 16. <sup>g</sup> Ref. 13.

### Figure Captions

FIG. 1: Detail of the  ${}^1Q_6$  branch of  ${}^{79}\text{Br}_2\text{O}$ . Some  $J$  assignments are given. The tightening of the quadrupole patterns with increasing  $J$  (up to 81) can be seen for  $J$  up to 60, when asymmetry splitting becomes prominent; + and - indicate the parity of levels. The band turns at  $J = 75$ ; the irregular appearance in this region is caused in part by  $\chi_{ab}$ , and the  $J$  assignments of near-degeneracies are also given and indicated by \*. See also text and Fig. 4. The P-branch near 414 GHz also belongs to  ${}^{79}\text{Br}_2\text{O}$ .

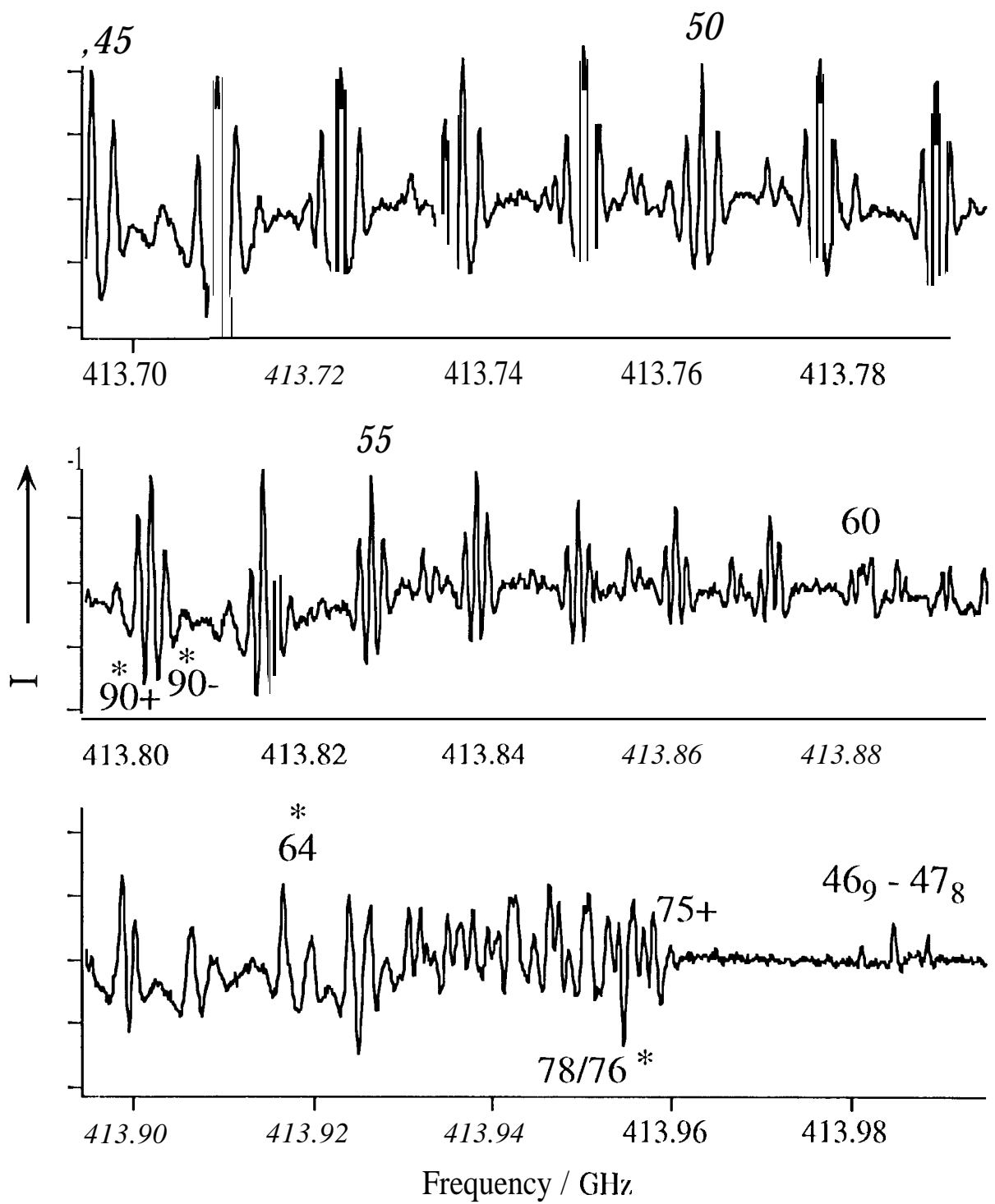
FIG. 2: The  $1127, 105 \rightarrow 1126, 106$  (left) and the  $1127, 106 \rightarrow 1126, 107$  transition of  ${}^{81}\text{Br}_2\text{O}$  (right) showing quadrupole splittings for high  $J$  transitions dominated by  $\chi_{-}$ . Note: the intensity ratios of ca. 1:4:1 and 3:4:3 are due to the spin-statistics, see text.

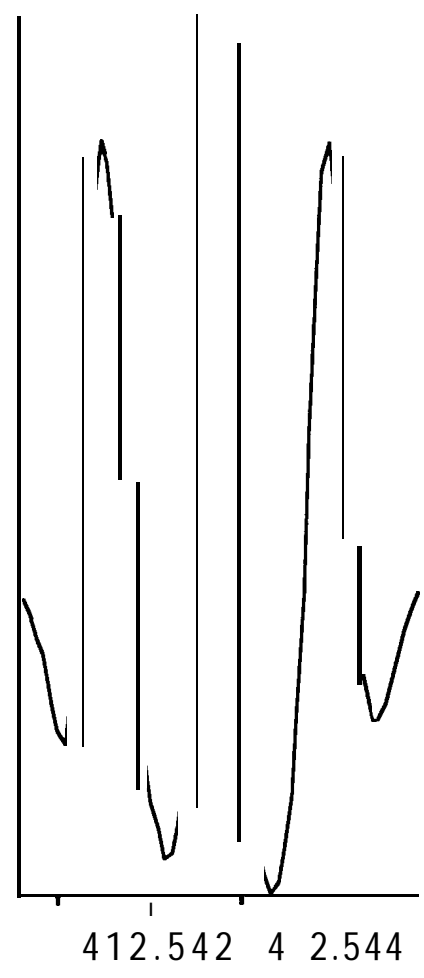
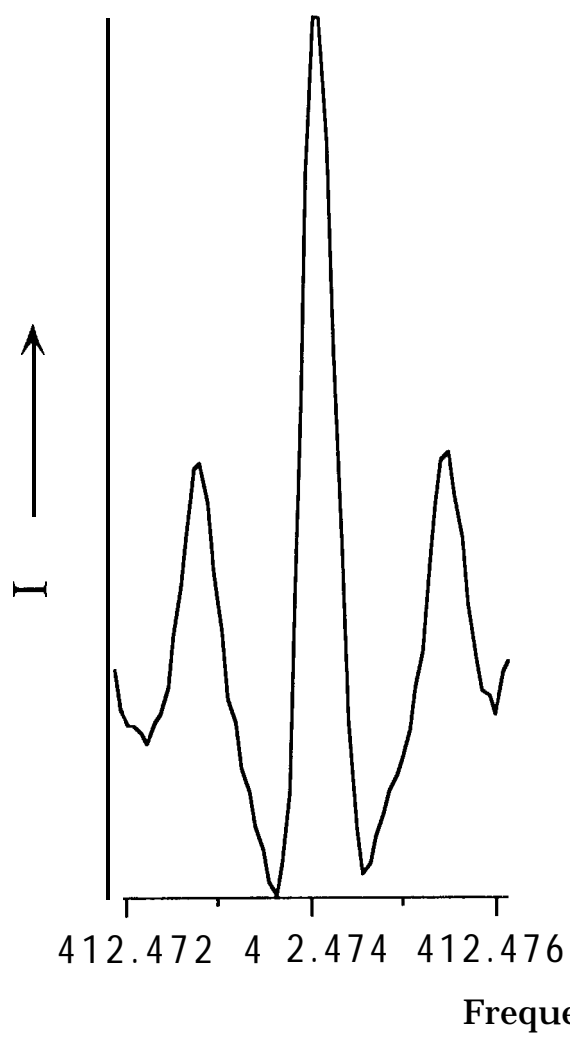
FIG. 3: The origin of the  $K_a = 7-6$  R-branch of  ${}^{81}\text{Br}_2\text{O}$ . The hyperfine pattern is dominated by  $\chi_{aa}$ . The lower state quantum numbers  $J$  and  $J'$  are indicated. Because of the spin-statistics there are only six of 16 strong hyperfine components with  $\Delta J = 1$  and  $J$  even for the  $7_{7,1} - 7_{6,0}$  transition and ten with  $J$  odd for  $7_{7,0} - 7_{6,1}$ .

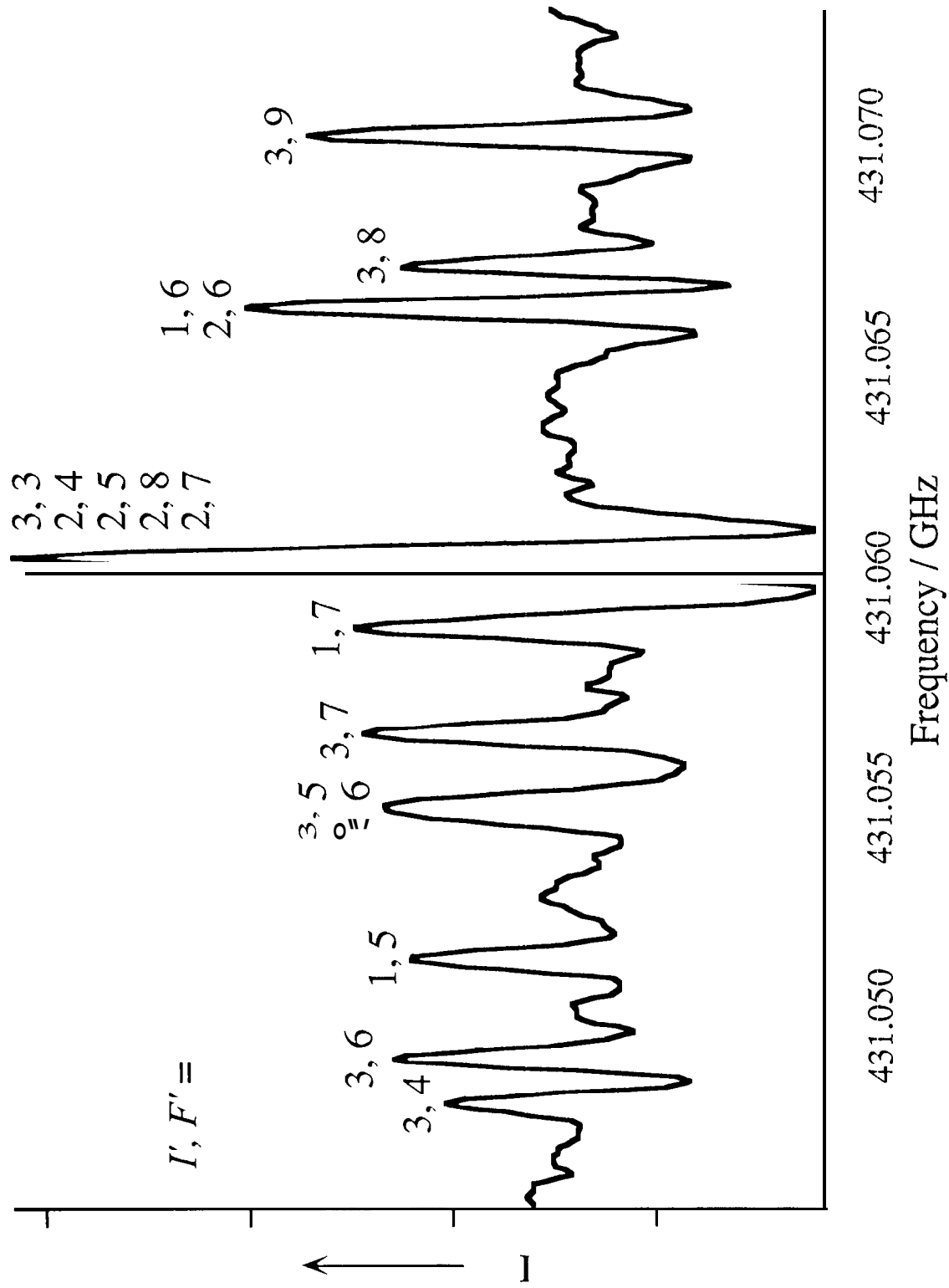
FIG. 4: The  $56_{5,52} - 55_{4,51}$  transition of  ${}^{81}\text{Br}_2\text{O}$ ; a) expected pattern without  $\chi_{ab}$ , b) observed pattern, c) simulated spectrum with  $\chi_{ab}$ . The energy difference between the unperturbed  $53_{5,49}$  and  $55_{4,51}$  levels is 874 MHz.

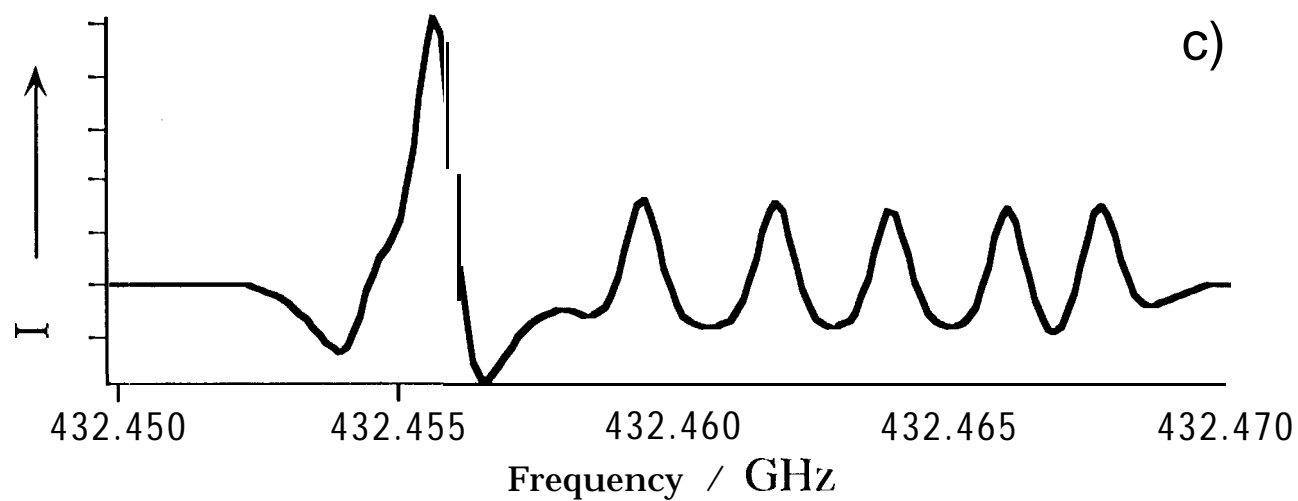
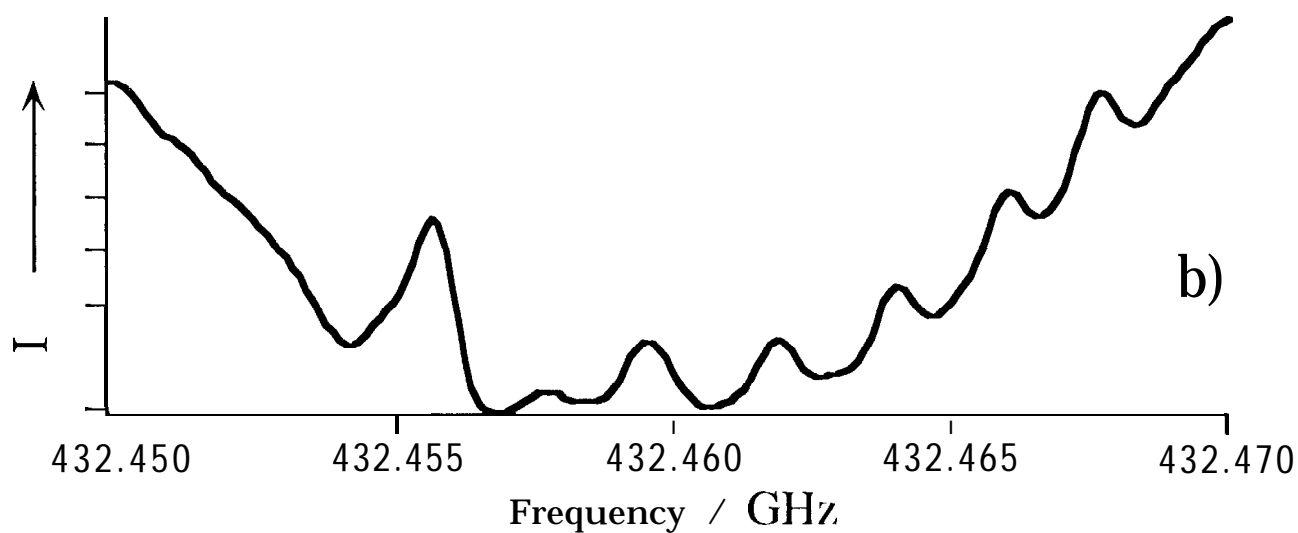
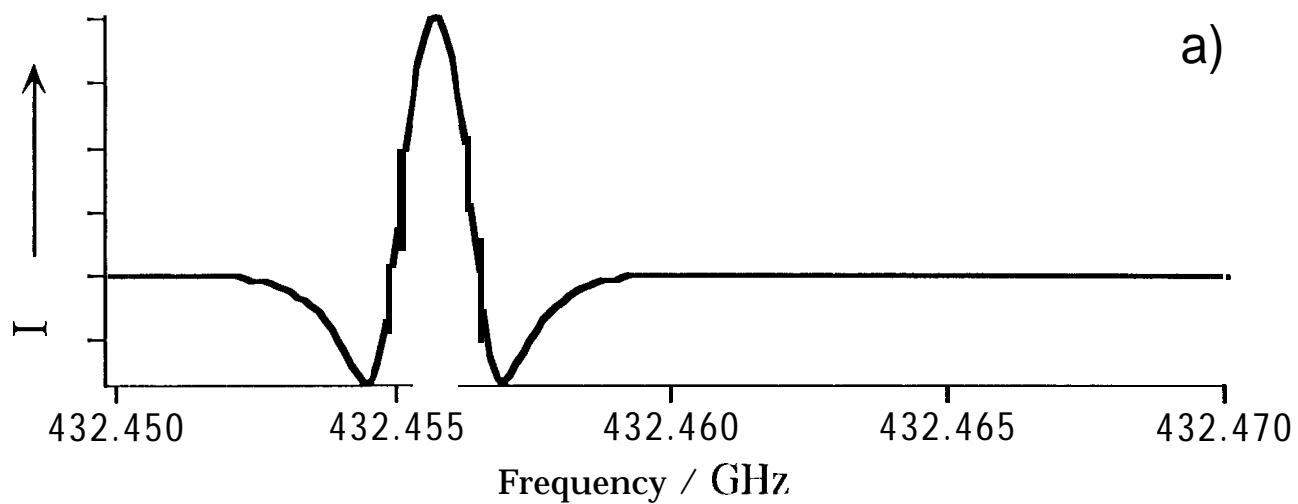
FIG. 5: Near-degeneracies of  $^{79/81}\text{Br}_2\text{O}$ .  $J$  of the larger  $K_a$  value *versus* the absolute value of  $AJ = 2$ ,  $\Delta K_a = -1$  energy difference is shown. Near-degeneracies accessed by transitions of  $^{79/81}\text{Br}_2\text{O}$  included in the fit are indicated by open circles. Measurable effects are encountered several  $J$ 's away from the value associated with the smallest energy difference; see also text.

FIG. 6: The principal inertial (dashed arrows) and quadrupole axis systems (solid arrows) of  $\text{Br}_2\text{O}$  ( $c = y$  is perpendicular to the molecular plane).











$J$  vs  $\Delta J=2, \Delta K_a=-1$  Intervals

